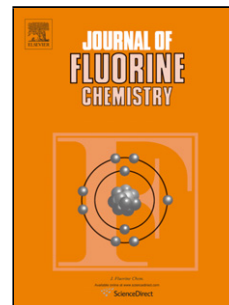


Accepted Manuscript

Title: Comparative Investigations on the Effects of Pendent Trifluoromethyl Group to the Properties of the Polyimides Containing Diphenyl-substituted Cyclopentyl Cardo-structure

Author: Xuemei Wang Feng Liu Jiancheng Lai Zhiqiang Fu Xiaozeng You



PII: S0022-1139(14)00118-3
DOI: <http://dx.doi.org/doi:10.1016/j.jfluchem.2014.04.016>
Reference: FLUOR 8312

To appear in: *FLUOR*

Received date: 1-3-2014
Revised date: 28-4-2014
Accepted date: 30-4-2014

Please cite this article as: X. Wang, F. Liu, J. Lai, Z. Fu, X. You, Comparative Investigations on the Effects of Pendent Trifluoromethyl Group to the Properties of the Polyimides Containing Diphenyl-substituted Cyclopentyl Cardo-structure, *Journal of Fluorine Chemistry* (2014), <http://dx.doi.org/10.1016/j.jfluchem.2014.04.016>

This is a PDF file of an unedited manuscript that has been accepted for publication. As a service to our customers we are providing this early version of the manuscript. The manuscript will undergo copyediting, typesetting, and review of the resulting proof before it is published in its final form. Please note that during the production process errors may be discovered which could affect the content, and all legal disclaimers that apply to the journal pertain.

Highlights

A fluorinated Cardo-type diamine was prepared.

The electron-withdrawing, hydrophobic and low-polarizable pendent CF_3 groups were introduced to the PIs.

The CF_3 groups led to desired reduction in CTC, coloration, water absorption and dielectric constant of PIs containing Cardo-structure.

Accepted Manuscript

Comparative Investigations on the Effects of Pendent Trifluoromethyl Group to the Properties of the Polyimides Containing Diphenyl-substituted Cyclopentyl Cardo-structure

Xuemei Wang ^a, Feng Liu ^{a*}, Jiancheng Lai ^b, Zhiqiang Fu ^a, Xiaozeng You ^{b*}

a. Department of Chemistry, Nanchang University, 999 Xuefu Avenue, Honggutan New District, Nanchang 330031, PR China

b. State Key Laboratory of Coordination Chemistry, School of Chemistry and Chemical Engineering, Nanjing National Laboratory of Microstructure, Nanjing University, Nanjing 210093, PR China

***. Correspondence authors:**

Feng Liu: liuf@ncu.edu.cn, tel (fax): (+) 86 791 83969984

Xiaozeng You: youxz@nju.edu.cn, tel (fax): (+) 86 25 83592969

Abstract: Two series of Cardo-type polyimides (PIs), fluorinated or nonfluorinated, were prepared from condensation of the fluorinated Cardo-type diamine 1,1-bis[4-(4-amino-2-trifluoromethylphenoxy)phenyl]cyclopentane (BATFPCP) or the analogous nonfluorinated Cardo-type diamine 1,1-bis[4-(4-aminophenoxy)phenyl]cyclopentane (BAPCP) with four aromatic dianhydrides PMDA, ODP, BTDA and BPDA, respectively. Both fluorinated and nonfluorinated PIs with Cardo-structure in polymer backbone generally retained good thermal properties comparable to aromatic PIs, with glass transition temperature (T_g) of 227-270°C and 234-340°C, 5% weight loss temperature in nitrogen (air) of 471-483°C (448-474°C) and 472-482°C (464-492°C), respectively. The fluorinated and nonfluorinated PIs with Cardo-structure in the polymer backbone showed tensile strengths of 90.1-101.7MPa and 78.6-99.6MPa, tensile modulus of 1.44-1.83GPa and 1.25-1.50GPa, respectively, also comparable to those of the traditional aromatic PIs. In comparison with nonfluorinated series, the fluorinated PIs possessed better solubility, higher optical transparency and lower water absorption. The fluorinated PIs were readily soluble in a variety of organic solvents, exhibited high optical transparency and light color with the cutoff wavelength at 373-424nm and transmittance at 500nm generally higher than 80%, and the water absorptions were measured as low as 0.18-0.93%. Additionally, the fluorinated series showed higher hydrophobicity by water contact angles and water absorption measurements and lower dielectric constant by dynamic dielectric measurements.

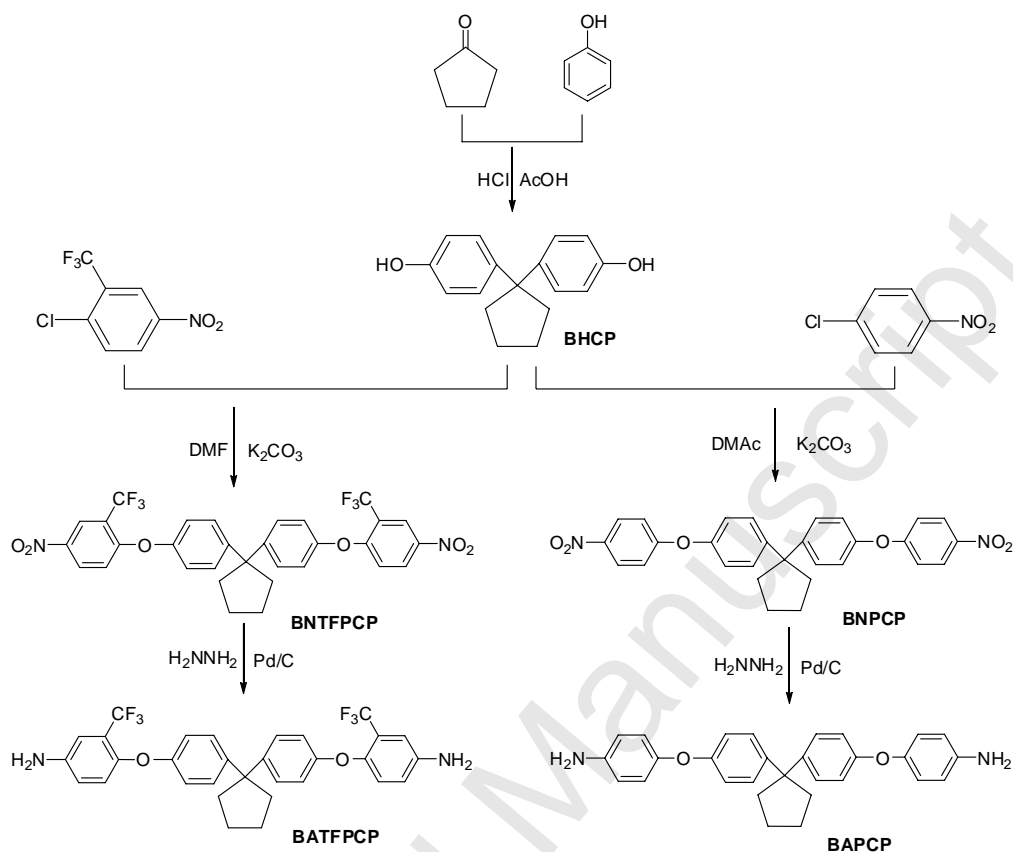
Key Words: polyimide, Cardo-structure, trifluoromethyl, structure-properties relationship

1. Introduction

Aromatic polyimides (PIs) have earned a reputation as high-performance materials in the aerospace and microelectronics industries in the form of films, moldings and reinforced composites, owing to their excellent thermal stability, good chemical and radiation resistance, mechanical and electrical properties [1,2]. However, aromatic PIs show poor processing performance such as high melting temperature and limited solubility in most organic solvents as a result of the rigid backbones which, together with highly conjugated aromatic structures and intermolecular charge transfer complex (CTC), further lead to intense coloration, reduced optical transparency and high dielectric constant, hence restricting their applications in optoelectronic and microelectronic fields such as flexible display and printed circuit board [3-5]. Polymer structure modification becomes necessary for such difficulties to be overcome. It has been reported that the enhancement of the practical properties like the tractability, optical and dielectric properties of PIs could be effectively achieved by introduction of flexible linkage, bulky substituents, and structurally unsymmetrical segments into the polymer backbone [6-8]. The main concepts behind these approaches lie in the reduction of conjugated aromatic characteristics and intermolecular interactions such as chain packing, charge transfer complex and electronic polarization interactions. Nevertheless, the improvements of these properties are usually obtained accompanied by the sacrifice of the inherent thermal and mechanical properties [9].

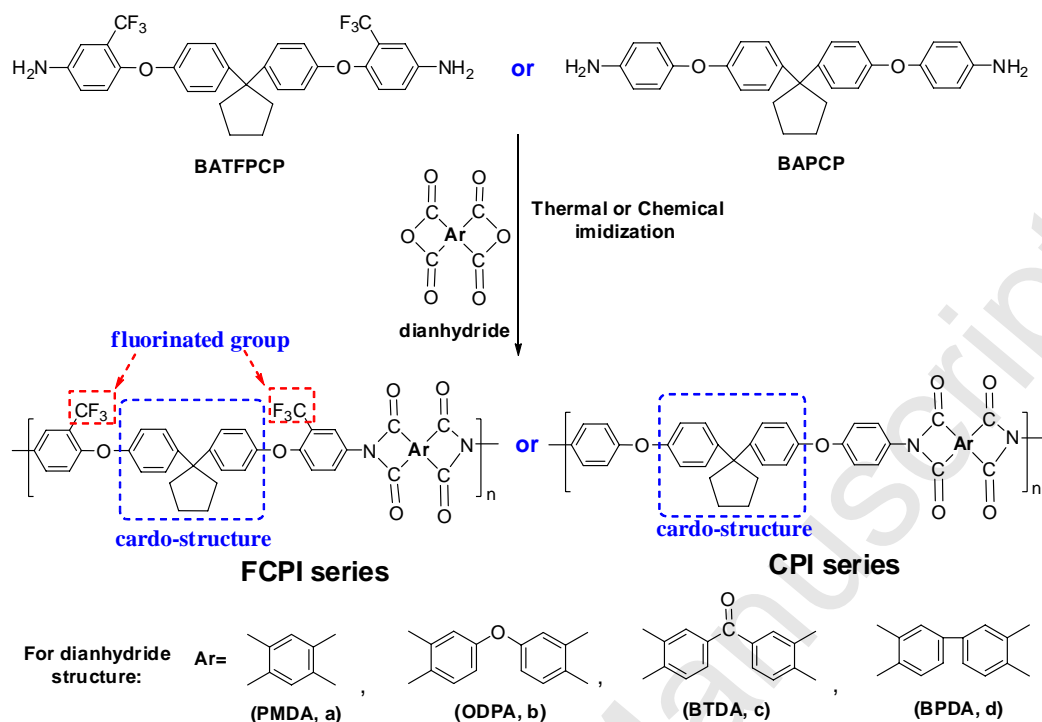
Of the strategies of polymer structure modification of PIs, the introduction of Cardo-structure into the polymer backbone stands out as it could upgrade the tractability of PIs by expanding the polymer interchain distance and reducing the polymer chain packing while essentially maintaining the thermal and mechanical properties of the PIs [10-13]. From the viewpoint of synthetic methodology, the Cardo-type structure could be incorporated into polymer backbone in terms of diamine or dianhydride monomers that are readily attained by reacting Cardo-type diol with the anhydride or amine precursor such as trimellitic anhydride, chlorophatic anhydride, or *p*-chloronitrobenzene with ester or ether linkage [14-17]. We have recently used this synthetic method to develop a series of alicyclic-functionalized PIs derivated from natural-(D)-camphor, which demonstrated better optical and dielectric properties than analogous aromatic PIs [18-20]. However, compared with the aromatic analogues, these alicyclic-functionalized PIs showed a reduction in thermal properties, which would hamper their applications where high-temperature fabrication processes are needed. As

a continuation, this piece of work was initiated to develop functional PIs, aiming at comprehensively evaluating the effect of the Cardo-structure and fluorinated functionality to the properties the polymers, with an emphasis on improving the tractability, optical and dielectric properties and simultaneously maintaining the inherent thermal and mechanical properties of PIs [21]. It was justifiably expected that the introduction of the bulky Cardo-structure into polymer backbone should play an important role in retaining the thermal properties and leading to the enhanced solubility as well. However, it has been worried that while the Cardo-structure helps improve the solubility of PIs by increasing the free volume, it may possibly result in an increase of moisture absorption that in turn increases the dielectric constant of PIs [22]. Herein we synthesized a diphenyl-substituted cyclopentyl Cardo-type diamine monomer with two pendent trifluoromethyl (CF_3) groups. We envisaged that the CF_3 groups would offset the negative effects of Cardo-structure in that it inhibits the moisture absorption due to its hydrophobic nature and further decreases the dielectric constant due to its low polarizability and the reduced moisture absorption [23-25]. Experimentally, the fluorinated Cardo-type diamine monomer 1,1-bis[4-(4-amino-2-trifluoromethylphenoxy)phenyl]cyclopentane (BATFPCP) and its nonfluorinated counterpart 1,1-bis[4-(4-aminophenoxy)phenyl]cyclopentane (BAPCP) were prepared starting from cyclopentanone through three steps, as shown in Scheme 1. The diphenol compound 1,1-bis(4-hydroxyphenyl)cyclopentane (BHCP) was synthesized from the reaction of cyclopentanone with excessive amount of phenol in the presence of hydrogen chloride and acetic acid as catalyst and 3-mercaptopropionic acid as co-catalyst. Aromatic nucleophilic substitution reaction of BHCP with 1-chloro-4-nitro-2-(trifluoromethyl)benzene or p-chloronitrobenzene in the presence of potassium carbonate afforded the intermediate dinitro compound 1,1-bis[4-(4-nitro-2-trifluoromethylphenoxy)phenyl]cyclopentane (BNTFPCP) or 1,1-bis[4-(4-nitrophenoxy)phenyl]cyclopentane (BNPCP). The following catalytic hydrogenation of the dinitro compounds of BNTFPCP or BNPCP by hydrazine monohydrate under Pd/C catalyst afforded the target diamine BATFPCP or BAPCP.



Scheme 1. The general synthetic route of BATFPCP and BAPCP

A series of fluorinated and analogous non-fluorinated PIs containing Cardo-structure were prepared by condensing BATFPCP or BAPCP with four aromatic dianhydrides PMDA, ODPDA, BTDA and BPDA, respectively, and the synthesized PIs were abbreviated as FCPI_a~FCPI_d or CPI_a~CPI_d correspondingly. The synthesis of the above PIs was shown in Scheme 2. All the PIs were subjected to the solubility, thermal, mechanical, optical, water absorption, and dielectric properties measurements for comparative structure-properties relationship studies.



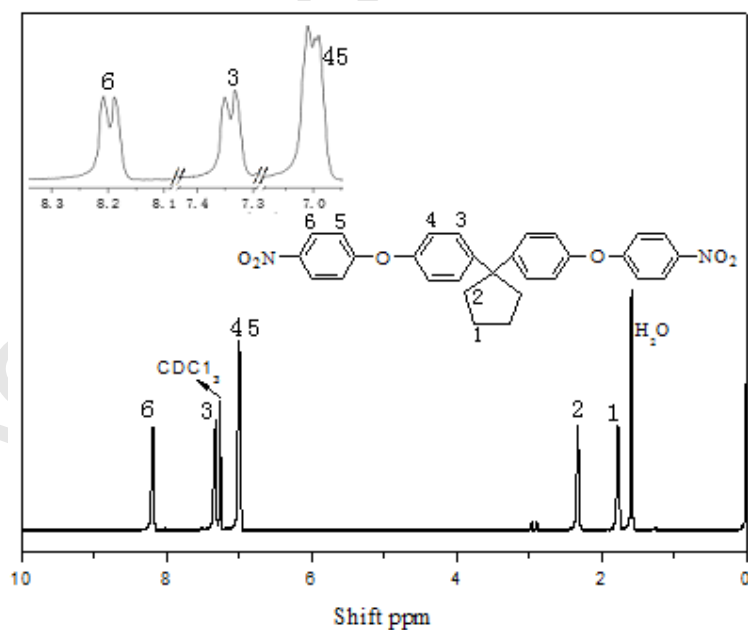
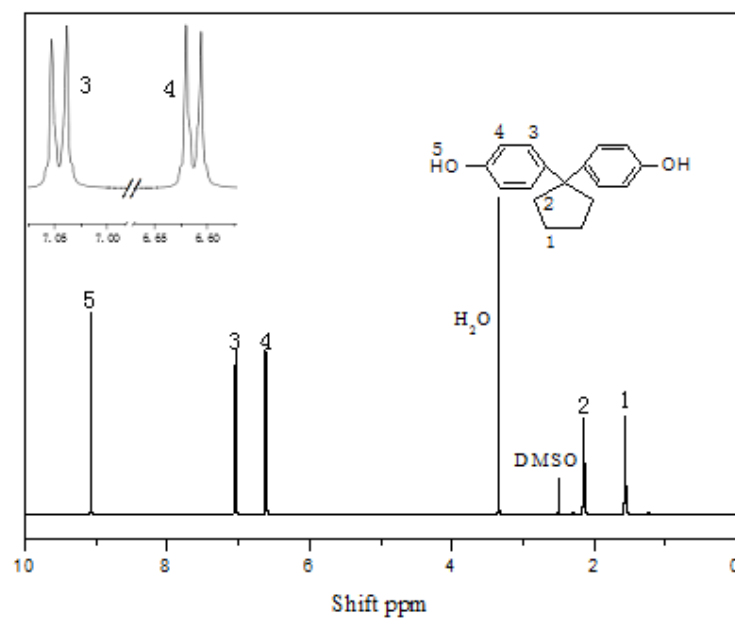
Scheme 2. The synthesis of fluorinated and nonfluorinated PI containing Cardo-structure (FCPI series and CPI series)

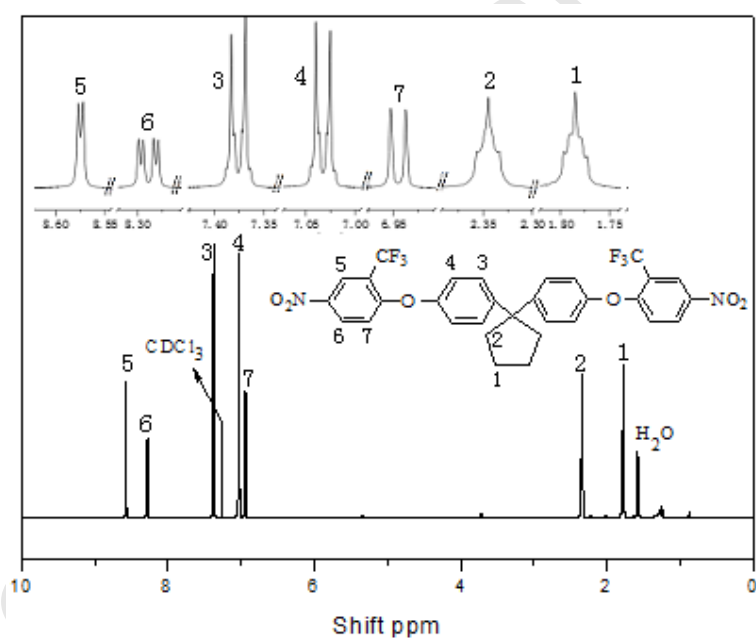
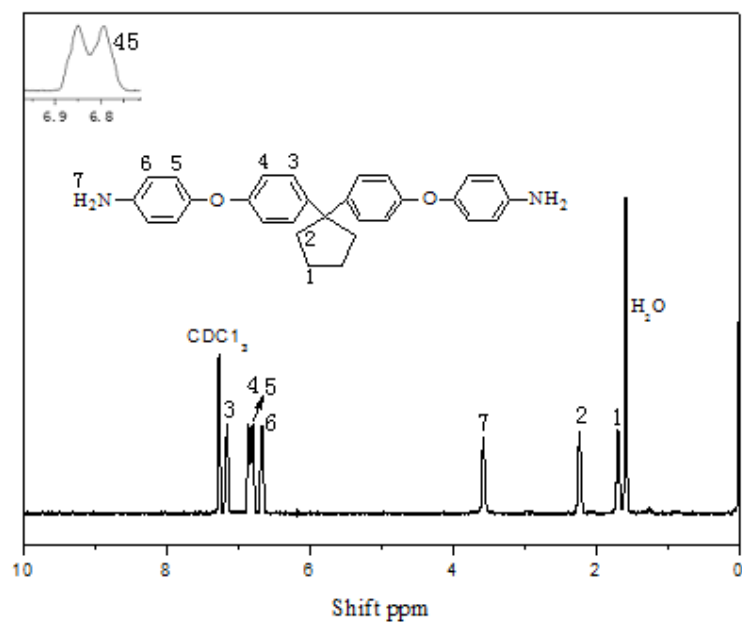
2. Results and discussion

2.1. Monomer synthesis

The structures of the intermediate and target products in each step were confirmed by IR spectra, ^1H NMR and ^{13}C NMR spectroscopy. As shown in Supporting Information (Figure S1), the nitro groups of compound BNTFPCP give two characteristic bands at 1535 and 1341 cm^{-1} corresponding to asymmetric and symmetric stretching of $-\text{NO}_2$. After the reduction, the characteristic absorptions of the nitro groups disappeared and the amino groups show a pair of N-H stretching bands at 3420 and 3356 cm^{-1} . Similarly, the absorption bands at 1508 and 1341 cm^{-1} attributed to asymmetric and symmetric stretching of the NO_2 groups in the dinitro compound BNPCP disappeared after the reduction, and the characteristic bands of the amino groups at 3433 and 3356 cm^{-1} appeared as corresponding to N-H stretching. In the ^1H NMR spectra in Fig. 1, the signals of aromatic and cyclopentyl protons of BNTFPCP appeared in the range of 6.94-8.57 and 1.74-2.34 ppm, and the signals of corresponding protons of BATFPCP were upfield shifted to 6.74-7.21 and 1.66-2.26 ppm. The proton H_5 of BNTFPCP resonated at the farthest downfield due to the inductive effect (-I effect) of

electron-withdrawing $-\text{NO}_2$ and $-\text{CF}_3$ groups, and the H_4 and H_7 *ortho*-oriented to the electron-donating ether (C-O) group shifted to the upfield as the result of +C effect. Similarly, the protons H_5 and H_6 of BATFPCP shifted to the upfield due to the electron-donating property of the amino group.





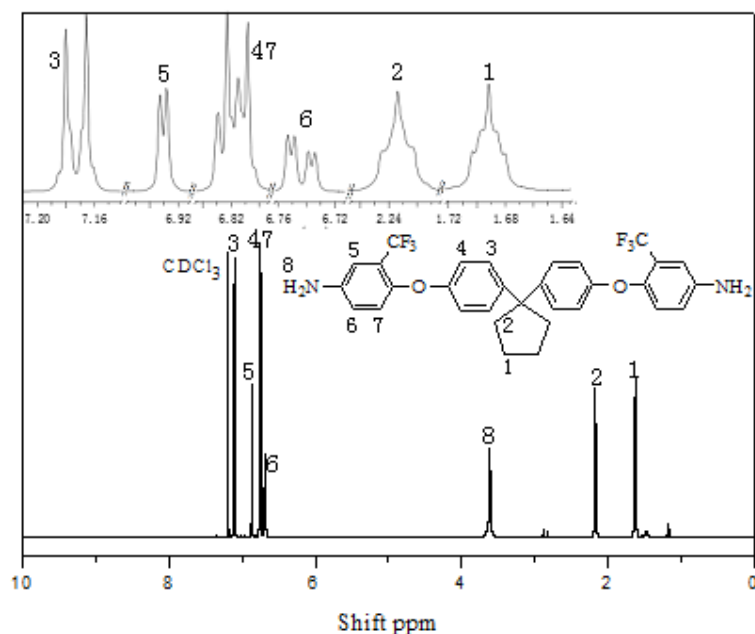


Fig. 1. The ¹H NMR spectra of the intermediate products and the diamine monomers.

In ¹³C NMR spectra in Supporting Information (Figure S2), both BNTFPCP and BATFPCP show a total of 14 main signals. BNTFPCP shows three quartets because of the heteronuclear ¹³C-¹⁹F coupling. The large quartet centered at about 122 ppm is attributed to the -CF₃ attached carbon. The single C-F (C¹⁴) couple constant in this case is 272 Hz. The CF₃-attached carbon (C⁹) also shows a clear quartet centered with a smaller coupling constant of 32.5 Hz due to C-F coupling. Also, the resonance of the C¹⁰ carbon (*ortho* to the CF₃ group) was split by the three fluorine atoms three-bond coupling. The close quartet has an even smaller coupling constant (5 Hz) because the interaction operated over more bonds. Similar splitting patterns (¹J_{C-F} = 272 Hz, ²J_{C-F} = 30 Hz and ³J_{C-F} = 5 Hz) are also found in the ¹³C NMR spectrum of BATFPCP. The spectra absorptions of BNPCP and BAPCP are similar to those of the reported cyclododecane-containing cardo-structure diamine [15], and slightly different chemical shifts of some peaks from the reported values could be attributed to their different Cardo-structures. These results clearly confirm that the diamines prepared herein are consistent with the proposed structure.

2.2 Polymer synthesis

The inherent viscosity of CPI_{a-d} and FCPI_{a-d} series were measured as 1.02, 0.94, 1.07, 0.98 dL/g and 0.92, 0.75, 0.82, 0.87 dL/g, respectively, which show that both BAPCP and BATFPCP display adequate condensation reactivity with the applied aromatic dianhydrides.

The characteristic absorption at 1383-1374 cm^{-1} attributed to C-N stretching and the absorption bands at about 1720 cm^{-1} and 1775 cm^{-1} attributed to asymmetrical and symmetrical stretching of imide carbonyl were observed in both fluorinated and nonfluorinated PIs with Cardo-structure, and the fluorinated series show the absorption at about 1260 cm^{-1} corresponding to characteristic C-F stretching of the pendent trifluoromethyl groups. Similar to those of the monomers, the +C effect of ether oxygen atoms linked with the two phenyl rings and -I effect and C-F coupling of the attached CF_3 groups could be observed in the ^1H NMR and ^{13}C NMR spectra of the resulting PIs. The representative IR and NMR spectra of FCPI_b were shown in Supporting Information (Figure S3).

2.3 Solubility and morphological structure of the polymers

The solubility behaviors of the chemically imidized PIs were investigated in various kinds of solvents by dissolving 100mg of powdery polymer samples in 2mL of the solvent either at room temperature or at elevated temperature, and the results are listed in Table 1. Generally, the PIs containing diphenyl-substituted cyclopentyl Cardo-structure show better solubility than traditional aromatic PIs [26, 27]. For instance, the introduction of the Cardo-structure made PIs soluble in the solvents other than polar solvents DMAc and NMP. It was found that the solubility of these PIs with Cardo-structure shows a correlation to the polymer backbone structures and pendant groups as well. The fluorinated polymers FCPI_b and FCPI_c showed excellent solubility in polar solvents such as NMP, DMF, DMAc and DMSO, and they were also soluble in low-boiling-point solvents such as CH_2Cl_2 and THF at room temperature or when heated, whereas, FCPI_a and FCPI_d showed slightly lower solubility. That could be attributed to the flexible molecular structure of ODPDA and BTDA corresponding to the dianhydride moiety of FCPI_b and FCPI_c and the comparably more rigid structure of PMDA and BPDA corresponding to the dianhydride moiety of FCPI_a and FCPI_d [28]. It is also seen that the fluorinated PIs showed better solubility in tested solvents than the analogous non-fluorinated PIs. That could be attributed to the presence of the bulky CF_3 group which increased the disorder in the chains and inhibited the dense chain packing, thus reducing the interchain interactions and enhancing the solubility of the PIs.

The morphological structure of the chemically imidized powdery PIs was analyzed by wide angle X-ray diffraction (WAXD) and illustrated in Supporting Information (Figure S4). It was observed that the synthesized fluorinated and nonfluorinated PIs both present a broad, low intensity peaks around $2\theta=15-20^\circ$, inferring that these polymers are completely

amorphous [29, 30]. That is reasonable because all the structures have the packing-disruptive diphenyl-substituted cyclopentyl Cardo-structure. It seemed that the nonfluorinated series display a wider reflection hump than the fluorinated series. According to Bragg's equation ($\lambda=2d\sin\theta$) [31, 32], one can calculate the mean intermolecular distance (d) from the peak maximum. The bigger calculated d values of fluorinated Cardo-type PIs (5.3879-5.7810 Å) compared with those of nonfluorinated Cardo-type PIs (4.9894-5.4672 Å) indicates a loose chain packing density of the fluorinated series. This result could be attributed to the steric hindrance and low polarizability of the pendent bulky CF_3 group that increases the free volume and accordingly reduces the polymer interchain interaction. These characteristics also endow desired properties with fluorinated series than nonfluorinated series such as lighter color in addition to higher solubility in solvents [33, 34].

Table 1.The solubility, *d*-spacing and optical properties of the PIs

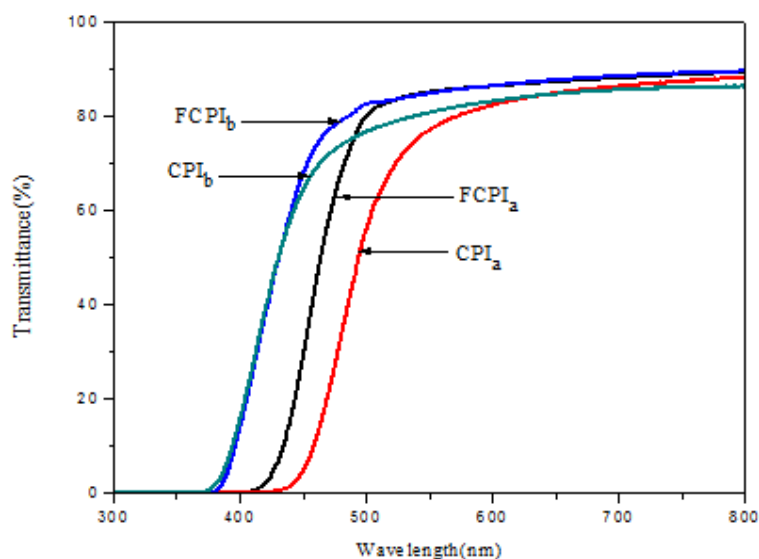
Codes	Solubility ^a							WAXD ^b		Optical Properties ^c		
	NMP	DMAc	DMF	DMSO	m-Cresol	THF	CH ₂ Cl ₂	2 θ (°)	<i>d</i> (Å)	λ_0 (nm)	T ₅₀₀ (%)	δ (μ m)
FCPI _a	++	+h	+h	--	--	--	--	16.439	5.3879	405	80.46	39
FCPI _b	++	++	++	++	++	++	++	16.036	5.5222	373	82.68	27
FCPI _c	++	++	++	++	++	+h	+h	16.210	5.4635	424	77.44	37
FCPI _d	++	+h	+h	+h	++	--	--	15.314	5.7810	398	82.94	40
CPI _a	--	--	--	--	--	--	--	17.762	4.9894	422	56.06	45
CPI _b	++	++	++	+h	++	+h	++	16.199	5.4672	373	76.81	34
CPI _c	++	+h	+h	+h	++	--	--	16.382	5.4064	441	50.27	45
CPI _d	+h	--	--	--	++	--	--	16.589	5.3394	398	80.80	51

^a Qualitative solubility measured with 100mg of the polymer in 2mL of solvent. ++, soluble at room temperature; +h, soluble when heated; --, insoluble even heated.

^b The *d* value is typical for the average chain-chain distance calculated from the prominent peak in WAXD pattern by Bragg equation. ^c λ_0 refers to the absorption edge from the UV-vis spectra of the polymer films, T₅₀₀ is the transmittance at 500nm in the UV-vis spectra, and δ is the measured thickness of the film samples.

2.4 Optical Properties of the polymers

Thin films of thermally imidized PIs were measured for optical transparency with UV-vis spectroscopy. Fig.2 shows the UV-vis transmittance spectra of the films, and the cut-off wavelength (λ_0) values and the percentage of transmittance at 500 nm from these spectra are listed in Table 2. It could be seen that the fluorinated series exhibited a λ_0 in the range of 373-424 nm, and the transparency at 500 nm (T_{500}) was higher than 77%. Apparently, the fluorinated series revealed lower λ_0 and higher optical transparency than their respective analogous nonfluorinated series [35]. The λ_0 could also be used to elucidate the color intensities of the PI films. It is clear that the values of λ_0 decrease in the order of $FCPI_c > FCPI_a > FCPI_d > FCPI_b$, and the color of these films changed in turn from dark yellow to colorless [36, 37]. The fact that fluorinated series showed lighter color than nonfluorinated series could be explained as attributed to the reduction of the intermolecular CTC between alternating electron-donating diamine moieties and electron-accepting dianhydride moieties [38]. The steric hindrance of pendent CF_3 groups enlarge the polymer interchain distances and the electron-withdrawing effect of attached CF_3 group decreases the electron-donating property of the diamine moieties [39], which together lead to the reduced interchain CTC formation of the fluorinated PIs.



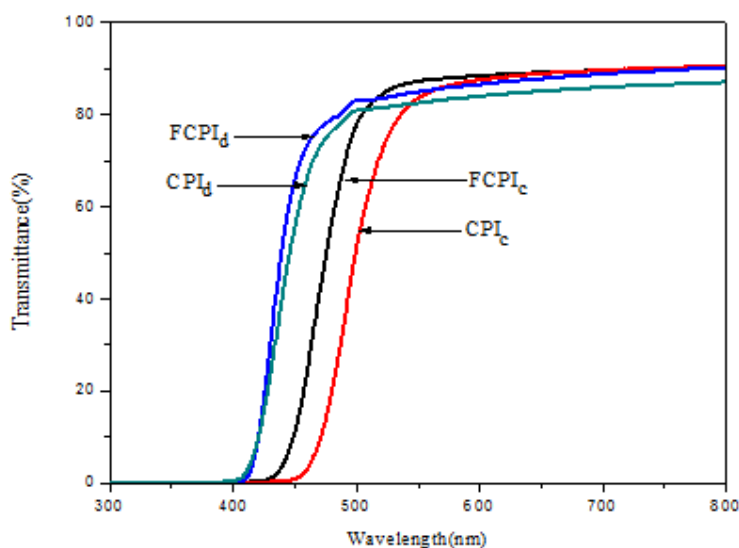


Fig. 2. Comparison of UV-visible spectra between FCPI series and CPI series.

2.5 Thermal Properties of the polymers

The thermal behaviors of the films of thermally imidized PIs were evaluated by dynamic mechanical analysis (DMA) and thermogravimetric analysis (TGA). The DMA curves of the PIs are shown in Fig.3 and the thermal analysis data from the DMA curves are summarized in Table 3. It can be seen that the PIs with Cardo-structure, either fluorinated or nonfluorinated, showed comparable thermal property as represented by the T_g values of FCPI series and CPI series in the range of 227-270°C and 234-300°C, respectively. It confirms that the introduction of Cardo-structure is one modification measure that could effectively retain the inherent thermal property of PIs. Apparently, as is reported, the T_g values of the fluorinated series were slightly lower than those of the unfluorinated series [40]. This would understandably be the result of the decreased electronic interchain interactions and loose dense packing caused by the low-polarizable bulky pendent CF_3 groups. The T_g values of these PIs show a dependence on the dianhydride component structure, and as expected, decrease with increasing flexibility of the polymer backbones in the dianhydride monomer order of PMDA > BPDA > BTDA > ODPA [41]. FCPI_b obtained from ODPA, for instance, shows the lowest T_g in fluorinated series because of the presence of a flexible ether linkage between every two phthalimide units. In the same manner, FCPI_a derived from PMDA, exhibits the highest T_g because of the rigidity of the polymer backbone.

Thermal decomposition of the PIs was evaluated by TGA in air or in nitrogen atmosphere at a heating rate of 10°C/min, and the typical TGA curves as represented by

FCPI_d and CPI_d are reproduced in Fig.4. The decomposition temperature at 5% and 10% weight loss (T_{d5} and T_{d10}) determined from the original TGA thermograms are listed in Table 3. The fluorinated series show good thermal stability and have no notable weight loss below 470°C. The values of T_{d5} of FCPI series are recorded in the range of 471-483°C in nitrogen and those of CPI series in the range of 472-482°C. The FCPI series left more than 51% char yield at 800°C in nitrogen except FCPI_a [42]. The TGA data indicates that these PIs with Cardo-structure, both fluorinated and nonfluorinated, possess fairly high thermal stability even with the introduction of the bulky CF₃ pendent groups [43].

These experimental results infer that the PIs containing the diphenyl-substituted cyclopentyl Card-structure in the polymer backbone, with or without fluorinated group, enjoy great thermal stability to withstand the harsh environments of many high-tech applications. The in-plane coefficients of thermal expansion (CTE) of the PIs were summarized in Table 3. The fluorinated PIs possess CTE values of 36.1-51.2 ppm/°C during the temperature scope of 25-300°C. The thermal stability of the fluorinated PI films as illustrated by CTE shows good consistence with the rigidity of the polymer chain. For example, FCPI_a obtained from PMDA, possesses the lowest CTE owing to the rigid structure of pyromellitic imide rings.

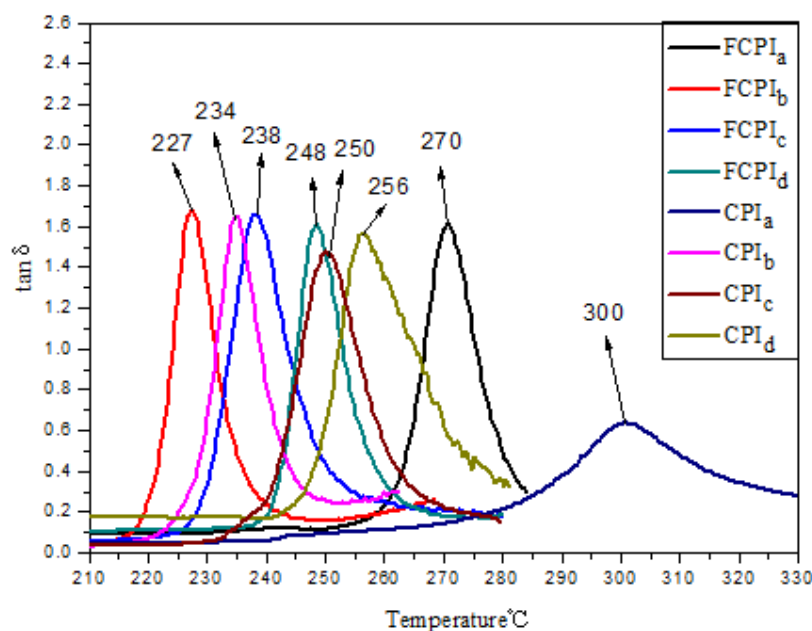


Fig. 3. Tan delta curves of the PIs by DMA technique.

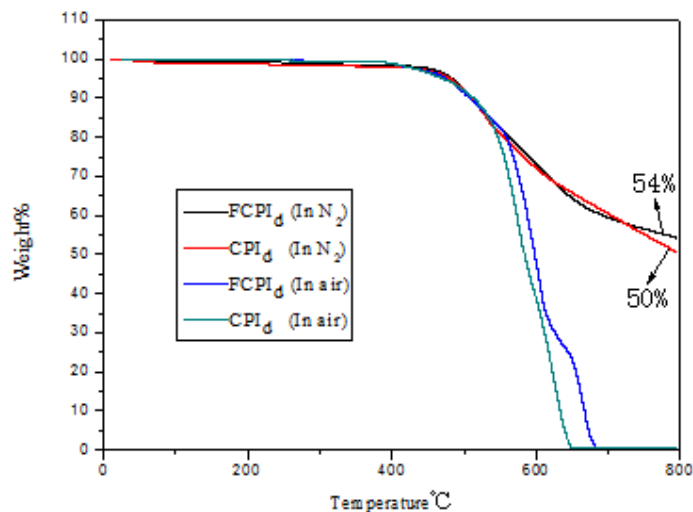


Fig. 4. TGA curves of FCPI_d and CPI_d.

2.6 Mechanical properties of the polymers

The films of thermally imidized PIs were subjected to tensile tests, and the results are summarized in Table 2. The fluorinated series show tensile strength at break of 90.1-101.7MPa, elongation at break of 12.7-14.2%, and initial modulus of 1.44-1.83GPa. The tensile properties of FCPI series are comparable with those of the CPI series. FCPI_a based on the aromatic dianhydride PMDA, exhibits low elongation at breakage of 12.7% due to the rigid polymer backbone. FCPI_b possesses the best mechanical properties with the elongation at break of 14.1% and tensile strength of 101.7MPa, which could be attributed to the presence of flexible ether linkage between two aromatic rings in the dianhydride moiety segment of ODPA [44]. Besides increased solubility and reduced color intensity, the pendent trifluoromethyl groups endow FCPI series with retained mechanical properties as compared with the non-fluorinated CPI series [45]. The difference between the tensile properties of the FCPI and CPI series seems slight and both series behave as strong and tough polymeric materials.

Table 2.

The thermal, mechanical, and surface, moisture uptake properties of the PIs.

Codes	Thermal properties						Mechanical properties ^d				γ_s (mN/m) ^f	Water absorption (%) ^g	
	T_g (°C) ^a	T_{d5} (°C)		T_{d10} (°C)		Char Yield (%) ^b	CTE (ppm/ °C) ^c	TM (GPa)	EB (%)	TS (MPa)			θ (°) ^e
		In N ₂	In air	In N ₂	In air								
FCPI _a	270	471	448	501	477	41	36.1	1.83	12.7	90.1	81.6	34.21	0.46
FCPI _b	227	483	455	510	499	51	44.1	1.55	14.1	101.7	80.9	34.78	0.20
FCPI _c	238	474	470	506	502	51	51.2	1.44	13.8	100.4	77.1	36.42	0.93
FCPI _d	248	482	474	509	507	54	42.1	1.49	14.2	95.0	84.5	32.62	0.58
CPI _a	300	481	466	504	504	34	32.3	1.25	12.0	78.6	74.1	38.57	0.89
CPI _b	234	482	492	504	512	48	40.3	1.33	12.6	98.6	78.2	36.03	0.32
CPI _c	250	472	464	507	498	39	45.0	1.28	10.4	92.2	75.9	37.96	1.02
CPI _d	256	479	470	509	512	50	36.2	1.50	14.6	99.6	74.5	38.82	0.73

^a Glass transition temperature (T_g) was measured by DMA at a heating rate of 10°C/min. ^b Residual weight percentage at 800°C in N₂. ^c The in-plane coefficients of thermal expansion. ^d TS: tensile strength; EB: elongation at break; TM: tensile modulus. ^e Equilibrium contact angle was measured at ambient temperature and double distilled water as solvent for a time period of 120 s depending on the stability of the drop, and the data was the average value of ten experiments. ^f Surface energy is obtained indirectly from the water contact angle by Owen equation. ^g Water absorption (%) = $(W - W_0 / W_0) \times 100$ %; where W is the weight of polymer sample after immersed in water for 96 h at room temperature and W_0 the weight of polymer sample after being dried in vacuum at 100°C for 8 h..

2.7 Contact angle, surface free energy and water absorption of the polymers

The contact angles (θ) of the thermally imidized PI films against water are listed in Table 3. Fig.5 depicted the profiles of a droplet on the FCPI and CPI series surface. Obviously, all the fluorinated FCPI series show larger contact angles than pure Cardo-type CPI series, and the θ of the two series are in the range of 77.1-84.5° and 70.1-78.2°, respectively. The results indicate that the presence of pendent trifluoromethyl group could strikingly increase the hydrophobicity of the Cardo-type PIs. With measured contact angles, surface energy can be calculated by the following equation: $1+\cos\theta=2(\gamma_s/\gamma_l)^{1/2}\exp[-\beta(\gamma_l-\gamma_s)]^2$ [46-48], where, β is a constant with a value of $0.0001247(\text{m}^2/\text{mJ})^2$, which is determined from contact angle data for low energy solids; γ_s and γ_l are the surface energy of the solid and the surface energy of the testing liquid, respectively. The calculated results of surface free energy in Table 2 show that the γ_s values of the fluorinated series present a corresponding decrease compared with those of pure Cardo-type PIs. Large contact angle and low surface free energy of the fluorinated series could mainly originate from the hydrophobic trifluoromethyl groups, which lead to the migration of the fluorocarbon chain segments to the film surface and fluorine enrichment at the surface, thus reducing the surface tension and making the surface more hydrophobic. Additionally, the hydrophobic trifluoromethyl groups inhibited the water absorption of the polymers [49]. As noted in Table 2, fluorinated series exhibit relatively low water uptakes. The values of moisture uptake for CPI series are in the range of 0.32-1.02%, whereas for FCPI series the values are shown to be smaller, ranging in 0.20-0.93%.

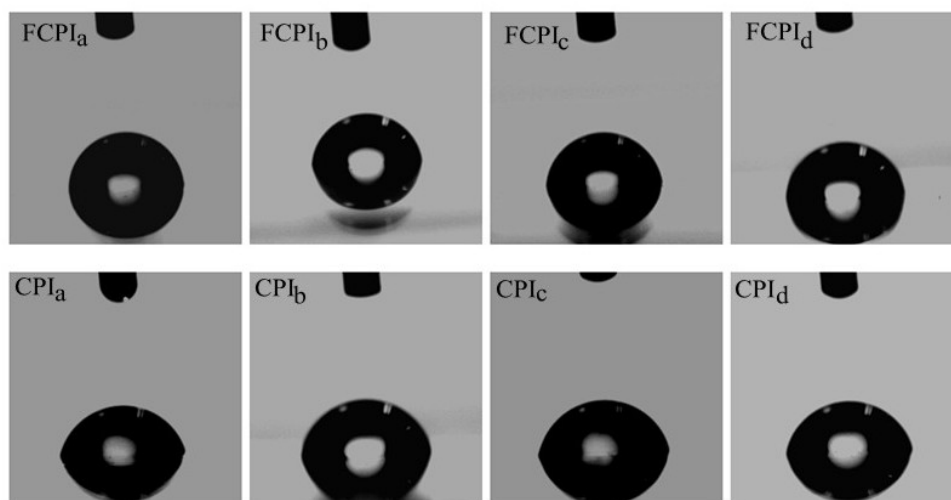
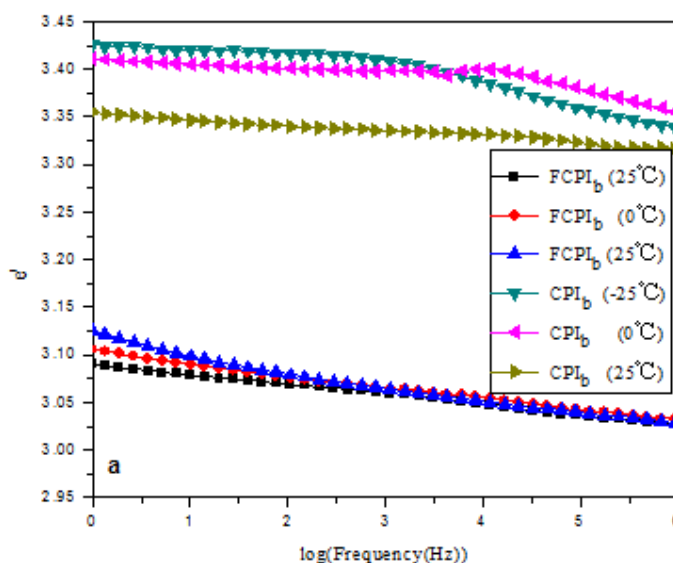


Fig. 5. Representative images of contact angles of the PI films.

2.8 Dielectric properties of the polymers

Dielectric properties of the thermally imidized PI films (FCPI_b and CPI_b) were evaluated on the basis of dielectric constant (ϵ'), dielectric loss (ϵ'') and their variation with frequency and temperature. Fig.6(a) shows the frequency dependence of the dielectric constant of the two samples at three selected temperatures (-25°C, 0°C, 25°C). It could be seen that the value of ϵ' of both polymers decrease gradually with increasing frequency [50]. The ϵ' depends upon the ability of the polarizable units in the polymer structure to orient fast enough to keep up with the oscillations of an alternating electric field. When the frequency increases, the orientational polarization would gradually lose pace with the changing frequency, and so the dielectric constant ϵ' begins to decrease. Fig.6(b) shows the temperature dependence of ϵ' at three different frequencies (1Hz, 1KHz, 1MHz). A gradual increase in ϵ' of FCPI_b was observed with the increase of temperature at fixed frequency, and this effect was more prominent at lower frequencies. The ϵ' variation with temperature of CPI_b after 300K (25°C) is the same as that of FCPI_b. It is explained that as the temperature increases, the polymer chain become more mobile and the dipoles become freer to respond to the applied field, and thus the dielectric constant increases as the polarization increases with increasing temperature [51]. However, the ϵ' variation with increasing temperature of CPI_b appears complicated below 25°C with an initial increase followed by a decrease, and the mechanisms behind this experimental observation are still under investigation.



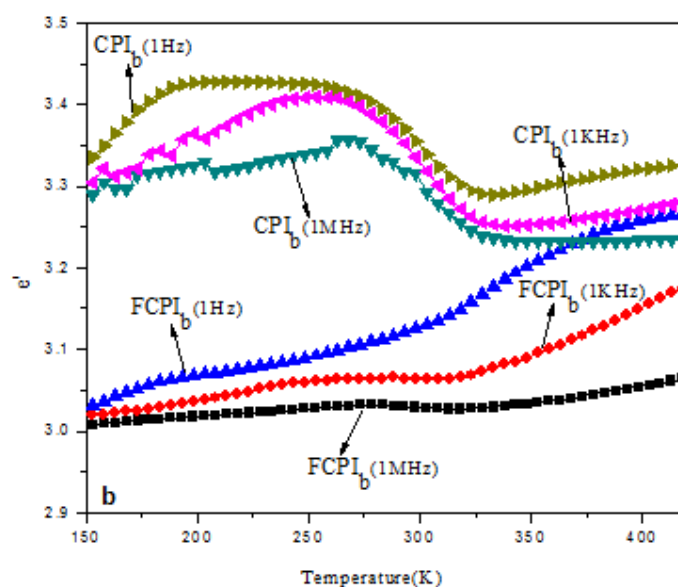


Fig. 6. (a). Dielectric constant (ϵ') vs. frequency of FCPI_b and CPI_b at selected temperatures. (b). Dielectric constant (ϵ') vs. temperature of FCPI_b and CPI_b at selected frequencies.

A general comparison of ϵ' and ϵ'' between FCPI_b and CPI_b at 25°C is presented in Table 3. Compared with traditional aromatic (PMDA-ODA) PI represented by Kapton whose dielectric constant (ϵ') was measured as about 3.68 at 1MHz at room temperature [52], the PIs with Cardo-structure represented by FCPI_b and CPI_b showed lower dielectric constant and thus displayed better potential for microelectronic application as the signal propagation velocity and fidelity are inversely related to the dielectric constant of the insulating material [22]. The dielectric constant of FCPI_b was in the range of 3.02-3.12, lower than those of CPI_b ranging in 3.31-3.35. The presence of pendent trifluoromethyl group in the diamine moiety segments contributes to the decrease the dielectric constant of fluorinated PI by three aspects. One is the reduced polarizability of polymer by strong electron-withdrawing inductive effect of trifluoromethyl group; secondary, the pendent fluorinated groups disturb the polymer chain packing and so lead to an increased free volume; additionally, the high hydrophobicity of trifluoromethyl group accordingly reduces the moisture content of fluorinated PI [53]. Meanwhile, low values of the dielectric loss (ϵ'') of the PIs containing Cardo-structure, both fluorinated and nonfluorinated, are indicative of minimal conversion of electrical energy into

heat in the dielectric material, and also advantageous for lowering the electrical signals loss in the dielectric medium.

Table 3

Comparison of ϵ' and ϵ'' of FCPI_b and CPI_b at selected frequencies and 25°C.

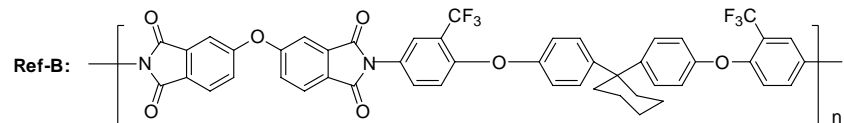
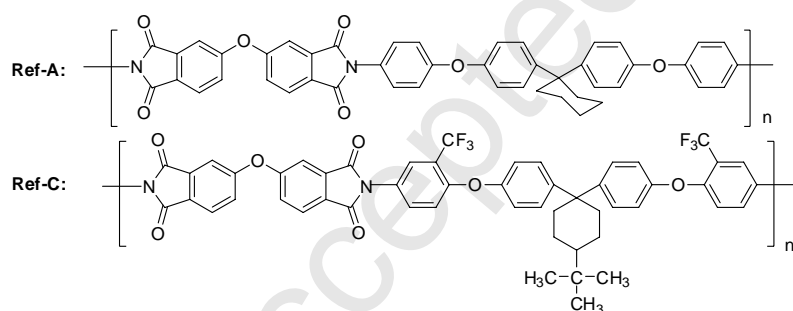
Polymer	Dielectric constants (ϵ')				Dielectric loss (ϵ'')	
	1Hz	100Hz	1KHz	1MHz	1Hz	1KHz
FCPI _b	3.12	3.07	3.06	3.02	0.0238	0.0096
CPI _b	3.35	3.34	3.33	3.31	0.0083	0.0035

2.9 General properties comparison between polymers in this work and those previously reported

Three previously reported structurally-similar PIs Ref-A, Ref-B and Ref-C, which were prepared from ODPAs condensed with cyclohexyl-containing Crado-type diamine 1,1-bis[4-(3,4-aminophenoxy)phenyl]cyclohexane, 1,1-bis[4-(4-amino-2-trifluoromethylphenoxy)phenyl]cyclohexane, and 1,1-bis[4-(2-trifluoromethyl-4-amino-phenoxy)phenyl]-4-tert-butylcyclohexane, respectively, have been used for properties comparison with the PIs in this work. Two PI films CPI_b and FCPI_b in this work have been used for comparison so that all the compared PIs were derived from the same dianhydride ODPAs. Table 4 lists the general properties of the pure Crado-type PIs of CPI_b and Ref-A, and the fluorinated Crado-type PIs FCPI_b, Ref-B and Ref-C. It can be observed from the solubility behavior data and the UV-vis cut-off wavelength (λ_0) values that CPI_b possesses better solubility and higher transparency than Ref-A, and that FCPI_b displays comparable solubility and optical properties with the analogous fluorinated films Ref-B and Ref-C. Particularly, cyclopentyl Crado-type PIs CPI_b and FCPI_b show an advantage over the analogous cyclohexyl Crado-type PIs Ref-A and Ref-B on two important properties T_g and elongation at break (EB), which may originate from the polymer backbone structural variation between the five-membered ring of cyclopentyl moiety and the six-membered ring of cyclohexyl moiety. Although having the comparable thermal properties with FCPI_b, Ref-C demonstrates inferior general mechanical properties possibly due to the presence of the extra *tert*-butyl group attached to the cyclohexyl ring. As can be seen from the measured dielectric constant (ϵ'), the cyclopentyl ring and cyclohexyl ring structure as well show to be more effective in bringing down the ϵ' value than the *tert*-butylcyclohexyl ring does. It indicates that the FCPIs prepared in this work are more suitable for microelectronic application due to the better combined practical properties.

Table 4General properties comparison of CPI_b and FCPI_b with the reported structurally-similar PIs

code	solubility					Optical properties		Thermal properties				Mechanical properties			Dielectric constant (ϵ')	
	NMP	DMAc	DMF	DMSO	THF	λ_0 (nm)	δ (μm)	T_g ($^{\circ}\text{C}$)	T_{d10} ($^{\circ}\text{C}$) In N ₂	T_{d10} ($^{\circ}\text{C}$) In air	Char Yield	TM (GPa)	EB (%)	TS (MPa)	1KHz	1MHz
CPI _b	++	++	++	+h	+h	373	34	234	504	512	48	1.33	12.6	98.6	3.33	3.31
Ref-A ^a	++	--	--	--	--	393	69	230	532	536	54	1.72	12	105	3.43	3.24
FCPI _b	++	++	++	++	++	373	27	227	510	499	51	1.55	14.1	101.7	3.06	3.02
Ref-B ^b	++	++	++	++	++	377	40	214	523	519	45	2.1	9	95	3.30	3.08
Ref-C ^c	++	++	++	+h	++	372	77	231	515	494	42	1.1	12	86	4.07	4.03



^a All the original data have been obtained from **Reference 14 and 15**. ^b All the original data have been obtained from **Reference 15**. ^c All the original data have been obtained from **Reference 21**.

3. Conclusion

This paper presented two series of PIs (FCPI series and CPI series) that were derived from the corresponding fluorinated and nonfluorinated diamines containing diphenyl-substituted cyclopentyl Cardo-structure (BATFPCP and BAPCP). It is demonstrated that the introduction of Cardo-structure into the PI's polymer backbone leads to better solubility, higher optical transparency and lower dielectric constant while retaining the thermal and mechanical properties generally comparable to those of aromatic PIs. Comparative studies reveal that the pendent CF_3 groups attached to the diamine moiety are shown to be effective to further inhibit the water absorption and reduce the dielectric constant of the PIs, owing to the synergistic effect of the decreased electron-donating properties of diamine moiety, increased steric hindrance, reduced polarizability and enhanced hydrophobicity. The eminent combination of the practical properties makes the resulting fluorinated PIs with cyclopentyl Cardo-structure (FCPI series) in this work potential competitive candidates for fabricating microelectronic devices.

Acknowledgements

The authors are thankful to the NSFC (Grant Nos. 51263014, 21271099 and 50803026), the Major State Basic Research Development Program (Grant No. 91022031) and Jiangxi provincial Education Department (Grant No. GJJ13113) for their financial support of this work.

4. Experimental

4.1 Materials

Cyclopentanone, 3-mercaptopropionic acid, 1-chloro-4-nitro-2-(trifluoromethyl)benzene, p-chloronitrobenzene, anhydrous potassium carbonate, 10% palladium on activated carbon (Pd/C), hydrazine monohydrate were of analytical purity grade and used as received. Pyromellitic dianhydride (PMDA), 3, 3', 4, 4'-oxydiphthalic anhydride (ODPA), 3, 3', 4, 4'-benzophenonetetracarboxylic dianhydride (BTDA), 3, 3', 4, 4'-biphenyltetracarboxylic dianhydride (BPDA) were recrystallized from acetic anhydride and dried in a vacuum oven at 150°C overnight prior to use. N, N-dimethylformamide (DMF), N, N-dimethylacetamide (DMAc) were purified by distillation under reduced pressure over phosphorus pentoxide and stored over 4\AA molecular sieves. Other commercially available materials were used without further purification.

4.2 Measurements

IR spectra were recorded on an Agilent Fourier Transform Infrared spectrometer FTS-40. ^1H NMR and ^{13}C NMR spectra were measured on Bruker DRX 400 spectrometers with CDCl_3 or $\text{DMSO}-d_6$ as the solvent and tetramethylsilane as the internal reference. The melting points were measured with a microscopic melting point meter SGW-X4. Elemental analyses were carried out on a Perkin-Elmer 2400 C, H, N analyzer. The inherent viscosities of the poly (amic acid) were measured with an Ubbelohde viscometer at 30°C at a concentration of 0.5 g/dL using DMAc as the solvent. Contact angle measurements were carried out by using Drop Master 300 Contact AM system (Kyowa Interface Science Co., Saitama, Japan). Wide-angle X-ray diffraction (WAXD) measurement were performed at 25°C on a Bede XRD Di system using graphite-monochromatized $\text{Cu-K}\alpha$ radiation ($\lambda=0.15405\text{nm}$). Ultraviolet visible (UV-vis) spectra of the polymer films were recorded on a Shimadzu UV-visible spectrophotometer UV-2450. Thermogravimetric analysis (TGA) were conducted with a Perkin-Elmer TGA-2 in flowing nitrogen or in air at a heating rate of $10^\circ\text{C}/\text{min}$. Dynamic mechanical analysis was conducted with DMA Q800 V20.22 Build 41 using tensile mode at the frequency of 1Hz. The stress-strain behavior of the PI film samples were tested by an Instron universal tester model 1122 (GB/T1040.1-2006) at room temperature with a stretching rate of 2.5mm/min, and the data was the average value of five experiments except for the maximum and the minimum value. Coefficients of thermal expansion (CTEs) of the films were detected in the optical dilatometer DIL-806 dilatometer (Baehr-Thermoanalyse GmbH, Germany) with the heating rate of 10K/min and measurement precision of 0.1 μm . Dielectric spectroscopy measurements of the PI films with the temperature variation in the range of 150-520 K and the frequency variation in the range of 1- 10^7 Hz have been performed using a Novocontrol Dielectric Spectrometer (GmbH Germany), CONCEPT 40.

4.3 The synthesis of the fluorinated and nonfluorinated Cardo-type diamine monomers

4.3.1 The synthesis of BHCP

A mixture of cyclopentanone (8.41g, 0.1mol), phenol (37g, 0.4mol), 3-mercaptopropionic acid (1.03mL), 90ml hydrochloric acid/ acetic acid (volume ratio 2:1) was placed in a 500mL three-necked flask equipped with a mechanical stirrer and reacted at room temperature for 24 h. The purple precipitate was washed with hot water and dissolved in 2mol/L aqueous sodium hydroxide solution, acidized with concentrated hydrochloride acid,

filtrated and washed with water, dried at 60°C under vacuum and recrystallized from toluene twice to afford pink crystals in 73.6 % yield (m. p.: 153-155°C). IR (KBr, cm^{-1}): 3253 (O-H stretching); 3033 (Ar-H stretching); 2969, 2866 (C-H Stretching). ^1H NMR (DMSO, δ , ppm): 9.08 (s, 2H, H₅), 7.05 (d, J = 8.6 Hz, 4H, H₃), 6.61 (d, J = 8.6 Hz, 4H, H₄), 2.14 (s, 4H, H₂), 1.57 (s, 4H, H₁). ^{13}C NMR (DMSO, δ , ppm): 156.27 (C⁷), 139.72 (C⁴), 128.69 (C⁵), 115.12 (C⁶), 54.28 (C³), 38.63 (C²), 22.84 (C¹). Elemental analysis (%): calculated: C, 80.28; H, 7.13; found: C, 80.26; H, 7.16.

4.3.2 The synthesis of BNTFPCP

To a three-necked round bottom flask of BHCP (2.54g, 0.01mol) and 1-chloro-4-nitro-2-(trifluoromethyl)benzene (4.74g, 0.021mol) completely dissolved in DMF was added potassium carbonate (4.14g, 0.03mol). The reaction was stirred at 100°C for 8 h, then cooled to room temperature and poured into water. The precipitate was washed with ethanol, recrystallized from DMF/water (volume ratio 1:1) and dried in vacuum at 60°C to afford white crystals in 87.1% yield (m. p.: 116-118°C). IR (KBr, cm^{-1}): 3097 (Ar-H stretching); 2981, 2866 (C-H Stretching); 1535, 1341 (-NO₂ stretching); 1263, 1160 (C-F and C-O stretching). ^1H NMR (CDCl₃, δ , ppm): 8.57 (d, J = 2.7 Hz, 2H, H₅), 8.29 (dd, J = 9.2, 2.7 Hz, 2H, H₆), 7.40-7.35 (m, 4H, H₃), 7.06-7.00 (m, 4H, H₄), 6.94 (d, J = 9.2 Hz, 2H, H₇), 2.34 (t, J = 6.8 Hz, 4H, H₂), 1.82-1.74 (m, 4H, H₁). ^{13}C NMR (CDCl₃, δ , ppm): 161.08 (C⁸), 151.92 (C⁷), 146.49 (C¹¹), 141.68 (C⁴), 129.76 (C⁵), 129.03 (C¹²), 123.91 (C¹⁰, quartet, $^3J_{\text{C-F}} = 5$ Hz), 123.88 (C¹⁴, quartet, $^1J_{\text{C-F}} = 272$ Hz), 120.36 (C⁹, quartet, $^2J_{\text{C-F}} = 32.5$ Hz), 120.09 (C⁶), 116.97 (C¹³), 56.28 (C³), 38.88 (C²), 22.91 (C¹). Elemental analysis (%): calculated: C, 58.87; H, 3.51; N, 4.43; found: C, 58.85; H, 3.51; N, 4.46.

4.3.3 The synthesis of BATFPCP

To a mixture of BNTFPCP (5g, 0.008mol), 10% Pd/C (0.3g), and 300mL ethanol in a three-necked flask was added hydrazine monohydrate (25mL) dropwise over a period of 0.5 h at 60°C. The reaction mixture was refluxing for 8 h. Filtration while hot to remove the catalyst and concentration using a rotation evaporator gave white solid, which was recrystallized from ethanol to afford BATFPCP with 86% yield (m. p.: 187-188°C). IR (KBr, cm^{-1}): 3420, 3356 (N-H stretching); 3051 (Ar-H stretching); 2969, 2866 (C-H Stretching); 1261, 1224, 1160, 1125 (C-F and C-O stretching). ^1H NMR (CDCl₃, δ , ppm): 7.21-7.15 (m, 4H, H₃), 6.93 (d, J = 2.8 Hz, 2H, H₅), 6.84-6.80 (m, 6H, H_{4,7}), 6.74 (dd, J = 8.7, 2.7 Hz, 1H, H₆), 3.71 (s, 4H, H₈), 2.26-2.18 (m, 4H, H₂), 1.75-1.66 (m, 4H, H₁). ^{13}C NMR (CDCl₃, δ ,

ppm): 156.87 (C⁷), 146.56 (C⁸), 143.46 (C¹¹), 142.16 (C⁴), 128.12 (C⁵), 124.17 (C¹⁴, quartet, ¹J_{C-F} = 272 Hz), 121.85 (C⁹, quartet, ²J_{C-F} = 30 Hz), 119.33 (C¹²), 117.34 (C¹³), 112.91 (C⁶), 123.0 (C¹⁰, quartet, ³J_{C-F} = 5 Hz), 54.75 (C³), 38.93 (C²), 22.96 (C¹). Elemental analysis (%): calculated: C, 65.03; H, 4.58; N, 4.89; found: C, 65.04; H, 4.55; N, 4.91%.

4.3.3.4 The synthesis of BNPCP

To the mixture of BHCP (5.08g, 0.02mol) and p-chloronitrobenzene (6.62g, 0.042mol) in DMAc in a three-neck round bottom flask was added potassium carbonate (8.28g, 0.06mol). The reaction was stirred at 150°C for 8 h, then cooled to room temperature and poured into water. The precipitate was washed with ethanol, recrystallized from DMF/water (volume ratio 1:1) and dried in vacuum at 60°C for 8 h to afford brown needle-like crystals in 81% yield (m. p.: 167-169°C). IR (KBr, cm⁻¹): 3097 (Ar-H stretching); 2969, 2866 (C-H Stretching); 1508, 1341 (-NO₂ stretching); 1250, 1172 (C-O stretching). ¹H NMR (CDCl₃, δ, ppm): 8.20 (d, J = 7.6 Hz, 4H, H₆), 7.34 (d, J = 7.3 Hz, 4H, H₃), 7.10-6.95 (m, 8H, H_{4,5}), 2.33 (s, 4H, H₂), 1.77 (s, 4H, H₁). ¹³C NMR (CDCl₃, δ, ppm): 163.37 (C⁸), 153.55 (C⁷), 146.78 (C¹¹), 142.62 (C⁴), 128.81 (C⁵), 126.94 (C¹⁰), 120.09 (C⁹), 117.09 (C⁶), 55.79 (C³), 38.94 (C²), 22.96 (C¹). Elemental analysis (%): calculated: C, 70.15; H, 4.87; N, 5.64; found: C, 70.17; H, 4.84; N, 5.63.

4.3.5 The synthesis of BAPCP

To a mixture of BNPCP (5g, 0.01mol), 10% Pd/C (0.3g), and 300mL ethanol in a three-necked flask was added hydrazine monohydrate (25mL) dropwise over a period of 0.5 h at 60°C. The reaction mixture was kept refluxing for 8 h. Filtration while hot to remove the catalyst and concentration using a rotation evaporator afforded pale yellow solid, which was recrystallized from ethanol to afford BAPCP with 85% yield (m. p.: 143-144°C). IR (KBr, cm⁻¹): 3433, 3356 (N-H stretching); 3059 (Ar-H stretching); 2969, 2878 (C-H Stretching); 1238, 1160 (C-O stretching). ¹H NMR (CDCl₃, δ, ppm): 7.15 (s, 4H, H₃), 6.82 (d, J = 22.8 Hz, 8H, H_{4,5}), 6.66 (s, 4H, H₆), 3.57 (s, 4H, H₇), 2.23 (s, 4H, H₂), 1.69 (s, 4H, H₁). ¹³C NMR (CDCl₃, δ, ppm): 156.57 (C⁷), 148.76 (C⁸), 142.72 (C¹¹), 142.53 (C⁴), 127.99 (C⁵), 121.10 (C⁹), 115.62 (C⁶), 115.22 (C¹⁰), 54.66 (C³), 38.93 (C²), 22.98 (C¹). Elemental analysis (%): calculated: C, 79.79; H, 6.46; N, 6.42; found: C, 79.79; H, 6.47; N, 6.40.

4.4 The synthesis of PIs

The synthesis of FCPIa is used as an example to illustrate the general process of

preparing the PIs.

4.4.1 Thermal cyclodehydration

Diamine BATFPCP (1g, 0.0017mol) was completely dissolved in 12.5mL dried DMAc in a 50mL flask, and the equimolar dianhydride PMDA (0.3810g, 0.0017mol) was added in one portion. The mixture was stirred at room temperature for 12 h to form a viscous poly (amic acid) (PAA) solution and then poured onto a glass plate, placed in an oven at 80°C for 5 h to remove the solvent. The semidried PAA film was further thermally imidized by sequential heating at 100°C for 1 h, 150°C for 1 h, 200°C for 1 h, 280°C for 2 h. A flexible polyimide film was stripped off from the glass surface by being soaked in boiled water.

4.4.2 Chemical imidization

PAA solution was prepared using the same synthetic method as that for the thermal imidization. Then a mixture of acetic anhydride and triethylamine (volume ratio 2:1) was added and reacted at 120°C for 4 h. The resulting solution was slowly poured into methanol/water (volume ratio 1:1) while stirring and the precipitate was washed thoroughly with methanol and hot water, and then dried in vacuum oven at 100°C for 12 h.

References

- [1] D. Wilson, H.D. Stenzenberger, P.M. Hergenrother, *Polyimides-Chemistry and Application*, New York: Blackie and Sons Ltd, 1990.
- [2] M.X. Ding, *Prog Polym Sci.* 32 (2007) 623-68.
- [3] M. Hasegawa, K. Horie, *Prog Polym Sci* 26 (2001) 259-335.
- [4] C.Y. Wang, X.Y. Zhao, G. Li, J.M. Jiang, *Colloid Polym Sci.* 289 (2011) 1617-1624.
- [5] S.H. Hsiao, C.T. Li, *J. Polym. Sci. Part A: Polym. Chem.* 37 (1999) 1435-1442.
- [6] T.S. Leu, C.S. Wang, *J. Appl. Polym. Sci.* 87 (2003) 945-952.
- [7] T.M. Long, T.M. Swager, *J. Am. Chem. Soc.* 125 (2003) 14113-14119.
- [8] Z.L. Wu, B.C. Han, C.H. Zhang, D.Y. Zhu, L.X. Gao, M.X. Ding, Z.H. Yang, *Polymer* 53 (2012) 5706-5716.
- [9] K. Wang, L. Fan, J.G. Liu, M.S. Zhan, S.Y. Yang, *J. Appl. Polym. Sci.* 107 (2008) 2126-2135.
- [10] D.J. Liaw, W.H. Chen, *Polymer* 44 (2003) 3865-3870.
- [11] D.J. Liaw, B.Y. Liaw, C.W. Yu, *J. Polym. Sci. Part A: Polym. Chem.* 38 (2000) 2787-2793.

- [12] Y.T. Chern, *Macromolecules* 31 (1998) 5837-5844.
- [13] D.J. Liaw, B.Y. Liaw, C.Y. Chung, *J. Polym. Sci. Part A: Polym. Chem.* 37 (1999) 2815-2821.
- [14] C.P. Yang, R.S. Chen, C.W. Yu, *J. Appl. Polym. Sci.* 82 (2001) 2750-2759.
- [15] C.P. Yang, Y.Y. Su, F.Z. Hsiao, *Polymer* 45 (2004) 7529-7538.
- [16] M. Hasegawa, K. Kasamatsu, K. Koseki, *Eur. Polym. J.* 48 (2012) 483-498.
- [17] M. Hasegawa, A. Tominaga, *Macromol. Mater. Eng.* 296 (2011) 1002-1017.
- [18] H.S. Zhang, J. Li, Z.L. Tian, F. Liu, *J. Appl. Polym. Sci.* 129 (2013) 3333-3340.
- [19] J. Li, H.S. Zhang, F. Liu, J.C. Lai, H.X. Qi, X.Z. You, *Polymer* 54 (2013) 5673-5683.
- [20] F. Liu, S.K. Zhu, Z.L. Tian, H.X. Qi, CN102276562A, 2011.
- [21] D.J. Liaw, C.C. Huang, W.H. Chen, *Macromol. Chem. Phys.* 207 (2006) 434-443.
- [22] G. Maier, *Prog. Polym. Sci.* 26 (2001) 3-65.
- [23] D.X. Yin, Y.F. Li, Y. Shao, X. Zhao, S.Y. Yang, L. Fan, *J. Fluorine Chem.* 126 (2005) 819-823.
- [24] I.K. Shundrina, T.A. Vaganova, S.Z. Kusov, V.I. Rodionov, E.V. Karpova, V.V. Koval, Y.V. Gerasimova, E.V. Malykhin, *J. Fluorine Chem.* 130 (2009) 733-741.
- [25] H. Behniafar, N. Sefid-girandehi, *J. Fluorine Chem.* 132 (2011) 878-884.
- [26] D.J. Liaw, B.Y. Liaw, *Polymer* 40 (1999) 3183-3189.
- [27] D.J. Liaw, B.Y. Liaw, *Macromol. Chem. Phys.* 200 (1999) 1326-1332.
- [28] C.L. Chung, S.H. Hsiao, *Polymer* 49 (2008) 2476-2485.
- [29] B. Benedikt, M. Gentz, L. Kumosa, P. Rupnowski, J.K. Sutter, P.K. Predecki, M. Kumosa, *Composites: Part A* 35 (2004) 667-681.
- [30] S.H. Hsiao, W.J. Guo, C.L. Chung, W.T. Chen, *Eur. Polym. J.* 46 (2010) 1878-1890.
- [31] S. Velioglu, M.G. Ahunbay, S.B. Tantekin-Ersolmaz, *J. Membr. Sci.* 417-418 (2012) 217-227.
- [32] H.W. Wang, R.X. Dong, H.C. Chu, K.C. Chang, W.C. Lee, *Mater. Chem. Phys.* 94 (2005) 42-51.
- [33] D. Bera, P. Bandyopadhyay, B. Dasgupta, S. Banerjee, *J. Membr. Sci.* 407-408 (2012) 116-127.
- [34] H. Behniafar, M. Sedaghatdoost, *J. Fluorine Chem.* 132 (2011) 276-284.
- [35] C.P. Yang, Y.Y. Su, M.Y. Hsu, *Polym Int.* 56 (2007) 415-425.
- [36] W. Jang, H.S. Lee, S. Lee, S. Chio, D. Shin, H. Han, *Mater. Chem. Phys.* 104 (2007) 342-349.
- [37] W. Jang, D. Shin, S. Chio, S. Park, H. Han, *Polymer* 48 (2007) 2130-2143.

- [38] Y. Liu, Y.H Zhang, S.W Guan, L. Li, Z.H. J, Polymer 49 (2008) 5439-5445.
- [39] C.Y. Wang, X.Y. Zhao, G. Li, J.M. Jiang, Polym. Degrad. Stab. 94 (2009) 1746-1753.
- [40] C.P. Yang, Y.C. Chen, S.H. Hsiao, W.J Guo, H.M. Wang, J. Polym. Res. 17 (2010) 779-788.
- [41] L.M. Tao, H.X. Yang, J.G. Liu, L. Fan, S.Y. Yang, Polymer 50 (2009) 6009-6018.
- [42] T. Ma, S.J. Zhang, Y.F. Li, F.C. Yang, C.L. Gong, J.J. Zhao, Polym. Degrad. Stab. 95 (2010) 1244-1250.
- [43] M. Ghaemy, F.R. Berenjestanaki, J. Fluorine Chem. 144 (2012) 86-93.
- [44] Z.Y. Ge, L. Fan, S.Y. Yang, Eur. Polym. J. 44 (2008) 1252-1260.
- [45] C.P. Yang, Y.Y. Su, W.J Guo, S.H. Hsiao. Eur. Polym. J. 45 (2009) 721-729.
- [46] Z.G. Luo, T.Y. He, H.J. Yu, L.Z. Dai, Macromol. React. Eng. 2 (2008) 398-406.
- [47] S. Loan, A.L. Cosutchi, C. Hulubei, D. Macocinschi, G. Loanid, Polym. Eng. Sci. 47 (2007) 381-389.
- [48] S.J. Park, H.S. Kim, F.L. Jin, J. Colloid Interf. Sci. 282 (2005) 238-240.
- [49] F.C. Yang, Y.F Li, T. Ma, Q.Q. Bu, S.J. Zhang, J. Fluorine Chem. 131 (2010) 767-775.
- [50] S. Chisca, V.E. Musteata, I. Sava, M. Bruma, Eur. Polym. J. 47 (2011) 1186-1197.
- [51] K.P. Yoo, M.J. Lee, K.H. Kwon, J. Jeong, N.K. Min, Thin Solid Films 518 (2010) 5986-5991.
- [52] S.R. Sheng, D.P. Li, T.Q. Lai, X.L. Liu, C.S. Song, Polym. Int. 60 (2011) 1185-1193.
- [53] M. Ree, K. Kim, S.H. Woo, H. Chang. J. Appl. Phys. 81 (1997) 698-707.

